20 October 1995

ELSEVIER

Chemical Physics Letters 245 (1995) 129–135

CHEMICAL PHYSICS LETTERS

Ab initio and DFT investigations of intramolecular hydrogen bonding in 1,2-ethanediol

Gábor I. Csonka [a], Nguyen Anh [a], János Ángyán [b], Imre G. Csizmadia [c]

[a] *Department of Inorganic Chemistry, Technical University of Budapest, 1521 Budapest, Hungary*
[b] *Laboratoire de Chimie Théorique, Université de Nancy I, B.P. 239, 54506 Vandoeuvre-les-Nancy, France*
[c] *Department of Chemistry, University of Toronto, Toronto, Ontario, Canada M5S 1A1*

Received 15 June 1995; in final form 15 August 1995

Abstract

HF and generalized gradient approximation density functional calculations at the BP and B3P levels, supplemented with a series of basis sets of increasing quality, are presented for the lowest energy conformer of 1,2-ethanediol. The critical point of the O...H interaction appears as a weak minimum in a slightly varying low-density electron gas. The 3D analysis shows that at small values of $|\nabla\rho|$ an elliptic lens shaped surface appears around this critical point.

1. Introduction

Theoretical studies of the 10 unique 1,2-ethanediol conformers show that the most stable conformers are the tGg^- and gGg^- conformers [1–4]. In these conformations an intramolecular O–H...O interaction is present. Experimental data also suggest the co-existence of two intramolecular hydrogen-bonded conformers in the gas phase [5] and in low-temperature Ar matrices [6]. The accurate measurement of the equilibrium structure of 1,2-ethanediol is difficult because of the presence of several stable conformations and the complicated tunneling motion of the two hydroxyl hydrogens [5,6]; thus reliable theoretical equilibrium geometries are the starting point for further investigations.

In this Letter we concentrate on the HO...H interaction in the tGg^- conformation of 1,2-ethanediol (Fig. 1). These interactions are present in sugars; however, they can be studied at a much higher level of theory in 1,2-ethanediol than in sugars. Theoretical studies for aldo-pyrano-hexoses show that tGg^- type of HO...H interactions appear frequently in the most stable conformations of the pyranose rings [7–10]. In this Letter the interactions of the hydroxyl groups are analyzed utilizing gradient vector field theory. The results of the 3D analysis of the norm of the electron density gradient $|\nabla\rho|$

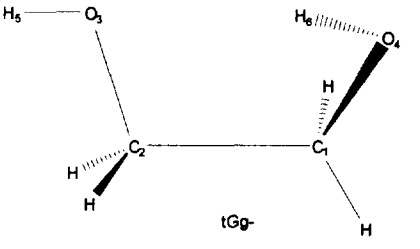

Fig. 1. Schematic representation of the tGg^- conformation of 1,2-ethanediol, where t is for $H_5-O_3-C_2-C_1$, G is for $O_3-C_2-C_1-O_4$ and g^- is for $C_2-C_1-O_4-H_6$ dihedral angle.

SSDI 0009-2614(95)00979-5

Table 1
The calculated critical points of the electron density in 1,2-ethanediol [a]

A	B	$r(A-B)$	$r_c(A)$	$r_c(B)$	ρ_c	$\nabla^2\rho_c$	ϵ_c	λ_1	λ_2	λ_3
HF/3-21G										
C1	C2	1.520	0.734	0.786	0.239	−0.639	0.050	−0.448	−0.426	0.235
C1	O4	1.436	0.551	0.885	0.226	−0.253	0.034	−0.360	−0.348	0.455
C2	O3	1.449	0.545	0.904	0.214	−0.203	0.015	−0.309	−0.305	0.411
H5	O3	0.965	0.233	0.732	0.332	−1.523	0.027	−1.457	−1.419	1.354
H6	O4	0.968	0.230	0.739	0.329	−1.558	0.029	−1.462	−1.422	1.325
HF/6-31G(d)										
C1	C2	1.514	0.742	0.772	0.275	−0.795	0.042	−0.570	−0.547	0.322
C1	O4	1.398	0.445	0.953	0.267	−0.165	0.011	−0.529	−0.524	0.888
C2	O3	1.408	0.446	0.962	0.256	−0.079	0.013	−0.483	−0.477	0.881
H5	O3	0.947	0.184	0.762	0.368	−2.097	0.022	−1.893	−1.852	1.647
H6	O4	0.949	0.183	0.766	0.366	−2.107	0.022	−1.898	−1.857	1.648
H6	O3	2.361	0.972	1.389	0.012	0.056	2.171	−0.011	−0.004	0.071
HF/6-31G(d, p)										
C1	C2	1.513	0.742	0.771	0.276	−0.799	0.040	−0.574	−0.551	0.325
C1	O4	1.397	0.445	0.952	0.268	−0.184	0.004	−0.535	−0.533	0.884
C2	O3	1.407	0.446	0.961	0.258	−0.097	0.021	−0.492	−0.482	0.878
H5	O3	0.942	0.181	0.761	0.393	−2.468	0.027	−2.088	−2.032	1.652
H6	O4	0.945	0.180	0.765	0.391	−2.485	0.027	−2.096	−2.041	1.652
H6	O3	2.366	0.974	1.392	0.012	0.056	1.695	−0.011	−0.004	0.071
HF/6-311G(d, p)										
C1	C2	1.512	0.740	0.772	0.275	−0.809	0.039	−0.565	−0.544	0.300
C1	O4	1.398	0.450	0.947	0.265	−0.148	0.012	−0.504	−0.498	0.854
C2	O3	1.407	0.451	0.956	0.255	−0.073	0.016	−0.462	−0.455	0.844
H5	O3	0.940	0.176	0.764	0.393	−2.903	0.025	−2.085	−2.035	1.217
H6	O4	0.942	0.174	0.768	0.391	−2.904	0.025	−2.093	−2.043	1.232
H6	O3	2.380	0.979	1.401	0.012	0.053	1.836	−0.011	−0.004	0.067
B3P/6-31G(d)										
C1	C2	1.515	0.745	0.769	0.262	−0.650	0.042	−0.517	−0.496	0.363
C1	O4	1.409	0.481	0.928	0.266	−0.498	0.017	−0.502	−0.494	0.498
C2	O3	1.422	0.483	0.939	0.254	−0.414	0.017	−0.455	−0.447	0.488
H5	O3	0.966	0.197	0.769	0.351	−1.839	0.021	−1.712	−1.676	1.549
H6	O4	0.971	0.195	0.776	0.346	−1.817	0.022	−1.697	−1.661	1.541
H6	O3	2.224	0.884	1.340	0.017	0.064	1.182	−0.017	−0.008	0.089
B3P/6-31G(d, p)										
C1	C2	1.514	0.746	0.768	0.263	−0.656	0.039	−0.521	−0.502	0.367
C1	O4	1.408	0.482	0.926	0.267	−0.522	0.014	−0.509	−0.502	0.489
C2	O3	1.421	0.484	0.938	0.255	−0.436	0.019	−0.464	−0.455	0.482
H5	O3	0.962	0.193	0.769	0.369	−2.086	0.027	−1.844	−1.795	1.554
H6	O4	0.967	0.192	0.776	0.364	−2.070	0.027	−1.833	−1.784	1.546
BP/6-31G(d)										
C1	C2	1.527	0.753	0.774	0.253	−0.588	0.040	−0.489	−0.470	0.371
C1	O4	1.425	0.507	0.918	0.259	−0.566	0.024	−0.487	−0.475	0.396
C2	O3	1.441	0.511	0.930	0.246	−0.491	0.024	−0.442	−0.432	0.383
H5	O3	0.977	0.204	0.774	0.340	−1.720	0.022	−1.609	−1.574	1.463
H6	O4	0.984	0.203	0.781	0.334	−1.686	0.022	−1.586	−1.552	1.452
H6	O3	2.217	0.877	1.340	0.017	0.062	1.119	−0.018	−0.008	0.088

Table 1 (continued)

A	B	$r(A-B)$	$r_c(A)$	$r_c(B)$	ρ_c	$\nabla^2\rho_c$	ϵ_c	λ_1	λ_2	λ_3
BP/6-31G(d, p)										
C1	C2	1.526	0.753	0.774	0.254	−0.594	0.036	−0.493	−0.476	0.375
C1	O4	1.425	0.509	0.916	0.260	−0.586	0.023	−0.495	−0.483	0.392
C2	O3	1.441	0.513	0.928	0.247	−0.509	0.023	−0.450	−0.440	0.380
H5	O3	0.974	0.200	0.774	0.357	−1.933	0.028	−1.723	−1.677	1.467
H6	O4	0.980	0.199	0.782	0.351	−1.903	0.028	−1.703	−1.657	1.456

[a] $r_c(A)$ and $r_c(B)$ are the distances (Å) from atoms A and B to the bond critical point respectively. ρ_c is the electron density (e/au^3), $\nabla^2\rho_c$ is the Laplacian of ρ_c, ε_c is the ellipticity of ρ_c and λ_i are the curvatures of the ρ_c at the bond critical point, respectively.

around the critical point of the HO...H interaction are visualized.

2. Computational methods

We use the following combinations of the generalized gradient approximation density functional (GGA-DFT) functionals:

(i) BP or Becke–Perdew method, in which Becke's exchange functional [11] is combined with Perdew's correlation functional [12].

(ii) B3P is a hybrid method. It is a linear combination of the HF, Slater and Becke exchange functionals and Perdew [11] correlation functional. The constants were determined by Becke by fitting heats of formations [13]. Note that Becke used the Perdew–Wang (PW91) functional instead of P86 [13].

The calculations were performed with GAUSSIAN 92/DFT [14] using a normal grid (50 radial shells, 194 angular points per shell, pruned to about 3000 points per atom) in the GGA-DFT calculations. The HF and GGA-DFT calculations were supplemented with 6-31G(d), 6-31G(d, p) and 6-311G(d) and 6-311G(d, p) basis sets [15]. We calculated the properties of the gradient vector field of the electron density, $\nabla\rho(\boldsymbol{r})$, by a modified version of the AIMPAC package [16] from the wavefunctions provided by the G92/DFT program. The former program was modified in our laboratory in order to perform 3D grid calculations. The visualization of the results was created by our programs (maps) written with the Explorer™ package. All calculations were performed on Silicon Graphics workstations.

3. Results and discussion

According to Van den Enden et al. [17] O...H nonbonded interactions can be classified into three major groupings. The electron density on a hydrogen-bond acceptor oxygen may be considered to concentrate on sp^3-, π- or σ-type orbitals. Our previous study showed that in the tGg^- conformation 1,2-ethanediol shows an sp^3-type interaction. Table 1 shows the results of the electron density analysis for this conformer. The position of the bond critical points (BCP), electron densities (ρ) and Laplacian of ρ ($\nabla^2\rho$) at the BCPs show characteristic behavior. The HF/3-21G results differ from all the other results. The position of the BCPs are closer to the oxygen atoms, and the electron densities in the BCPs are considerably smaller than in the HF/6-31G(d) or (d, p) calculations. This explains the earlier observations that the HF/3-21G geometries usually agree well with the experimental or correlated geometries [15]. This relatively poor basis set compensates the bond shortening effects in the HF method arising from the overconcentrated electron densities in the bond centers. The HF/6-31G(d), 6-31G(d, p) and 6-311G(d, p) electron densities in the BCPs show this overconcentration clearly (Table 1). The B3P and BP results show that the electron density in the BCPs decrease considerably as the electron correlation is introduced (Table 1). The BP method introduces a stronger correlation effect than the B3P method (the latter involves exact HF exchange) and thus provides lower electron densities in the BCPs and longer bond distances. The O3...H6 interaction results in a smaller electron density and less negative Laplacian in the BCP of the C2–O3 bond than in the BCP of the C1–O4 bond (Table 1). The same inter-

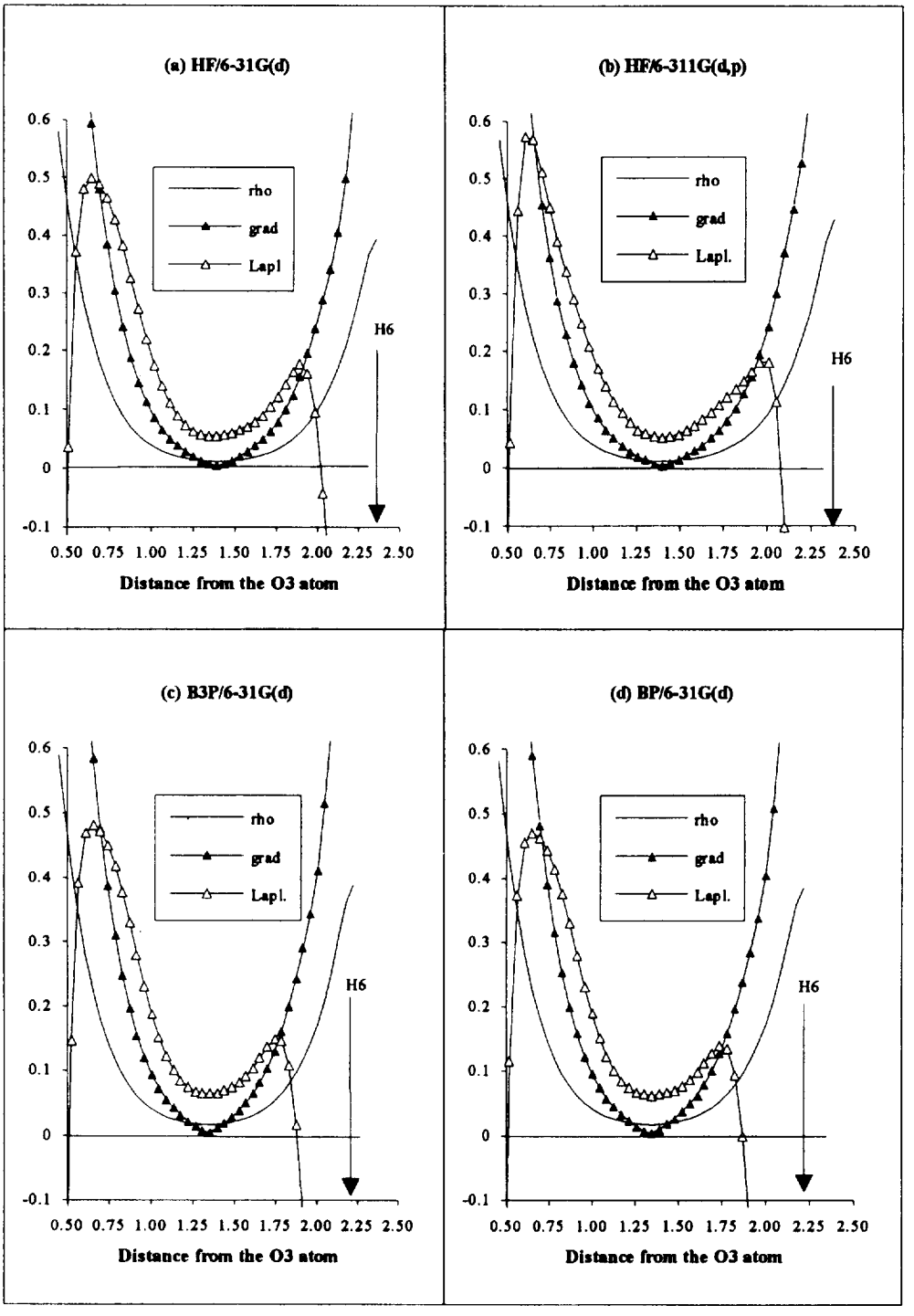

Fig. 2. The calculated electron densities (rho), the gradient of the electron densities (grad) and the Laplacians of rho (Lapl.), (all quantities are in au) versus the distance (Å) from the O3 atom in the direction of the H6 atom in the tGg^- conformer of 1,2-ethanediol. The position of the H6 atom is marked by an arrow.

action results in a longer H6–O4 bond length with smaller electron density, and more negative Laplacian in the BCP than for the H5–O3 bond. The positions of the BCPs are shifted toward the C1 ⇒ O4 ⇒ H6 direction. All methods yield consistently the same trends, but the O3...H6 interaction is less evident from the HF results.

The abovementioned effects suggest that an O3...H6 interaction is present in the tGg^- conformer of 1,2-ethanediol, however, the real proof would be a BCP between the O3 and H6 atoms (with a corresponding ring critical point). However, the AIMPAC program [16] did not find any critical points between the O3 and H6 atoms. The searches from various starting points were unsuccessful. This is because these critical points appear as a weak minimum in a slightly varying low-density electron gas. Under these circumstances the location of a minimum is difficult to find with the usual algorithm and precision. To illustrate the difficulties we plotted the values of the electron density, its gradient norm and Laplacian along the line connecting the O3 and H6 atoms in Fig. 2. The figure shows that there is a low density region at the 1.25–1.75 Å distance from the O3 atom. The true critical point is not in Fig. 2 because it is slightly off the line. The characteristics of the lowest gradient points along this line are given in Table 1 for the HF, B3P and BP methods. This interaction shows a similarity to the weak bonds in the charge-transfer complexes described earlier [18]. The large ellipticity (Table 1) is possibly caused by the merging of a BCP with a ring critical point. This critical point is similar to the O...H critical point found by us previously in aldo-pyrano-hexoses (in this critical point $\rho = 0.011$ au and $\nabla^2\rho = 0.065$ au) [10].

To analyze this interaction in three dimensions we wrote an Explorer map to visualize the norm of the electron density gradient, $|\nabla\rho|$, calculated at grid points around the molecule. From these pictures the regular BCPs may easily be identified as small spheres centered around the critical points at small $|\nabla\rho|$ values. Because of the grid noise the regular BCPs disappear at small $|\nabla\rho|$ values, however, the large volumes with small $|\nabla\rho|$ remain visible. This behavior can be used for the visualization of the properties of $|\nabla\rho|$ between the O3 and H6 atoms for the tGg^- conformation of 1,2-ethanediol.

Fig. 3 shows the low gradient (low electron density) gap between the O3 and H6 atoms at the

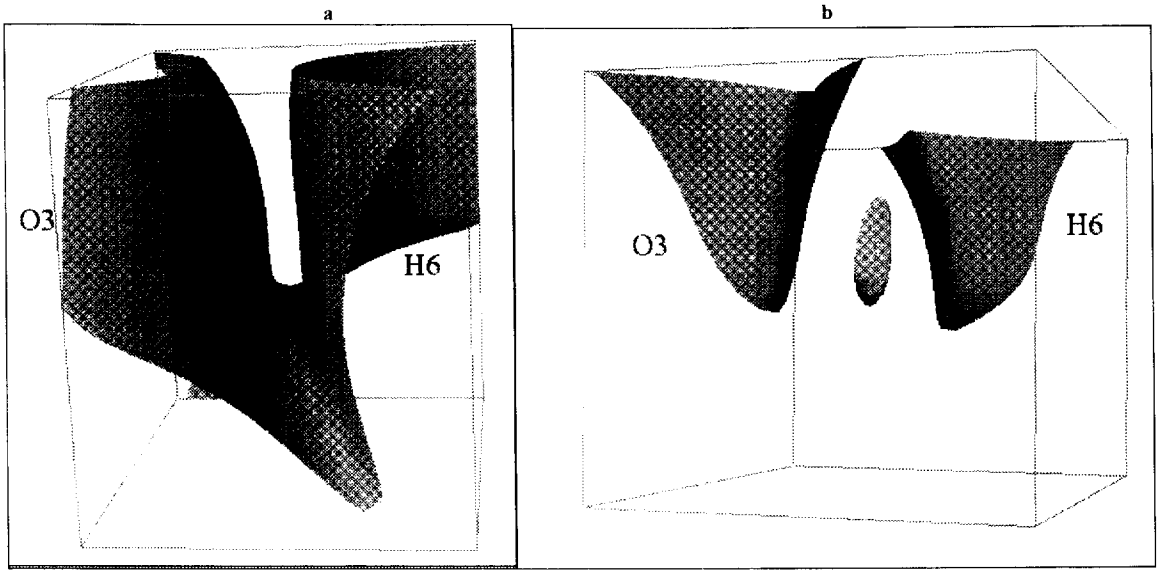

Fig. 3. 3D surfaces of the absolute value of the electron density gradient, $|\nabla\rho|$, at the HF/6-31G(d) level of theory for the tGg^- conformation of 1,2-ethanediol. The $|\nabla\rho| = 0.02$ au surface for the space between O3 (left) and H6 (right) is labeled as a and the $|\nabla\rho| = 0.0062$ au surface between O3 and H6 is labeled as b.

HF/6-31G(d) level of theory ($|\nabla\rho| = 0.020$ au, in Fig. 3a and $|\nabla\rho| = 0.0062$ au in Fig. 3b). Fig. 3a shows a smaller part of the 3D surface covering the molecule and it is interesting to see how these small $|\nabla\rho|$ points follow the molecular shape (the O3 atom is on the left and the H6 atom is on the right-hand side of Figs. 3a and 3b). Fig. 3a shows how large the $|\nabla\rho|$ gap is between the O3 and H6 atoms at $|\nabla\rho| = 0.020$ au value. If we decrease further the value of $|\nabla\rho|$ the volume of the gap decreases gradually, and for a value of 0.007 au the two surfaces merge. At a value of 0.0062 au an elliptic lens shaped closed surface appears around the critical point between the O3 and H6 atoms (Fig. 3b). Outside this closed surface $|\nabla\rho|$ is larger than 0.0062 au. The ellipticity of the point is visible from the figure. This is a new kind of visualization of the weak bonds in charge-transfer complexes. It should be noted that the HF and GGA-DFT methods provide qualitatively the same figures independent of the basis set applied, only minor quantitative differences appear between the various methods.

We also studied the electrostatic potential map projected to the 0.002 au electron density surface at the HF/6-31G(d) level of theory. From the map it was evident that the negative potential of the O3 lone pair at the H6 side is significantly smaller than the negative potential values of any other oxygen lone pairs in the tGg^- conformer. The positive potential on the H6 surface is also significantly smaller than on the H5 surface. This is further evidence for charge-transfer between the O3 and H6 atoms.

4. Conclusions

The following conclusions can be drawn from the above discussion.

(1) The results of the electron density analysis for the tGg^- conformer of 1,2-ethanediol show that the HF/6-31G(d), 6-31G(d, p) and 6-311G(d, p) methods overconcentrate the electron density in the BCPs. The electron correlation introduced by the B3P and BP methods decrease the electron density in the BCPs considerably. The relatively poor HF/3-21G method also provides low electron density in the BCPs, however, the results are quantitatively different from the correlated results.

(2) The critical point of the electron density between the O3 and H6 atoms for the tGg^- conformer of 1,2-ethanediol appears as a weak minimum in a slightly varying low density (0.012–0.017 au) electron gas. The critical point is characterized by a small positive Laplacian (0.053–0.064 au) and large ellipticity, possibly caused by the merging of a BCP with a ring critical point. The 3D analysis shows that at small values of $|\nabla\rho|$ an elliptic lens shaped surface appears around this critical point. This is a new kind of representation of the weak bonds in charge-transfer complexes. The charge-transfer is supported by the investigation of electrostatic potential maps.

Acknowledgement

The financial support of the Hungarian Research Foundation (OTKA T14975 and T16328) and the Balaton Project (No. 52) is acknowledged. The continuous financial support of the Natural Sciences and Engineering Research Council (NSERC) is gratefully acknowledged.

References

[1] B.J. Treppen, M. Cao, R.F. Frey, C. Van Alsenoy, D.M. Miller and L. Schäfer, J. Mol. Struct. THEOCHEM 314 (1994) 169.
[2] C.J. Cramer and D.G. Truhlar, J. Am. Chem. Soc. 116 (1994) 3892.
[3] T. Oie, I.A. Topol and S.K. Burt, J. Phys. Chem. 98 (1994) 1121.
[4] G.I. Csonka and I.G. Csizmadia, Chem. Phys. Letters 243 (1995) 419.
[5] P.-E. Kristiansen, K.-M. Marstokk and H. Mollendal, Acta Chem. Scand. A 41 (1987) 403.
[6] H. Takeuchi and M. Tasumi, Chem. Phys. 77 (1983) 21.
[7] P.L. Polavarapu, C.S. Ewig, J. Comput. Chem. 13 (1992) 1255.
[8] U. Salzner and P. von R. Schleyer, J. Org. Chem. 59 (1994) 2138.
[9] C.J. Cramer and D.G. Truhlar, J. Am. Chem. Soc. 115 (1993) 5745.
[10] G.I. Csonka, I. Kolossváry, P. Császár and I.G. Csizmadia, submitted for publication.
[11] A.D. Becke, Phys. Rev. A 38 (1988) 3098.
[12] J.P. Perdew, Phys. Rev. B 33 (1986) 8822.
[13] A.D. Becke, J. Chem. Phys. 98 (1993) 5648.

[14] M.J. Frisch, G.W. Trucks, M. Head-Gordon, P.M.W. Gill, M.W. Wong, J.B. Foresman, B.G. Johnson, H.B. Schlegel, M.A. Robb, E.S. Replogle, R. Gomperts, J.L. Andres, K. Raghavachari, J.S. Binkley, C. Gonzalez, R.L. Martin, D.J. Fox, D.J. DeFrees, J. Baker, J.J.P. Stewart and J.A. Pople, GAUSSIAN 92/DFT, Revision F (Gaussian, Pittsburgh, 1993).

[15] W.J. Hehre, L. Radom, P. von R. Schleyer and J.A. Pople, Ab initio molecular orbital theory (Wiley, New York, 1986), and references therein.

[16] R.F.W. Bader's laboratory, AIMPAC, McMaster University, Hamilton. ON L8S 4M1, Canada.

[17] L. Van den Enden, C. Van Alsenoy, J.N. Scarsdale and L. Schäfer, J. Mol. Struct. THEOCHEM 13 (1983) 471.

[18] J. Cioslowski, S.T. Mixon and W.D. Edwards, J. Am. Chem. Soc. 113 (1991) 1083.